Heat transport and the nature of the order parameter in superconducting UPt_3

M. R. Norman
Materials Science Division, Argonne National Laboratory, Argonne, Illinois 60439

P. J. Hirschfeld
Department of Physics, University of Florida, Gainesville, Florida 32611
(Received 11 September 1995)

Recent thermal conductivity data on the heavy fermion superconductor UPt_3 have been interpreted as offering support for an E_{2u} model of the order parameter as opposed to an E_{1g} model. In this paper, we analyze this issue from a theoretical standpoint including the detailed effects of Fermi surface and gap anisotropy. Our conclusion is that although current data put strong constraints on the gap anisotropy, they cannot definitively distinguish between these two models. Measurements on samples of varying quality could be decisive in this regard, however.

Well over a decade after the discovery of heavy fermion superconductivity, the pairing mechanism and even the order-parameter symmetry in these compounds remain controversial. Early suggestions of pairing in an unconventional superconducting state, based primarily on analysis of transverse ultrasound measurements in UPt_3,[1] were bolstered more recently by the discovery of a complex phase diagram for this system in applied magnetic field and pressure.[2] (Here we take ''unconventional'' to imply the existence of additional broken symmetries beyond the usual gauge U(1) broken in classic superconductors.[3])

Several current Ginzburg-Landau (GL) theories of the UPt_3 phase diagram attribute the existence of multiple superconducting phases to two nearly degenerate superconducting states, either (i) split by a symmetry-breaking field, such as the ordered antiferromagnetic moment in the basal plane, or (ii) ''accidentally'' degenerate.[2] Such theories can at the same time describe qualitatively the anisotropy of the superconducting state, insofar as the GL parameters can be chosen to stabilize an order parameter at low temperatures and fields which allows for a larger number of quasiparticle excitations with wave vector in the basal plane. Such a state is strongly indicated by analyses[4,5] of both ultrasound[1] and thermal conductivity measurements.[6,7] Beyond this crude statement, little is known for certain about the exact anisotropy or even the symmetry of the superconducting state of UPt_3.

Recently, Lussier *et al.*[7] have argued that thermal conductivity measurements can shed further light on these questions. They showed that the electronic heat current dominates the phononic current down to low temperatures for their high-quality samples, and that the relaxation rate $1/\tau_k$ in the normal state is nearly isotropic. Furthermore, their measurements imply the existence of large anisotropy in the superconducting state which does not simply reflect normal state anisotropy; together with transverse ultrasound measurements, these data provide convincing evidence for a highly anisotropic gap in UPt_3.

In order to determine the actual gap anistropy for UPt_3, it is necessary to go further and attempt to model the data. While it has been stated that such fits to transport properties cannot be expected to fix the detailed anisotropy due to uncertainties in the form of the impurity scattering amplitude, Fledderjohann and Hirschfeld[8] argued recently that ratios of transport coefficients should lead to more robust conclusions since they can depend only weakly on the relaxation times. They therefore focused on the ratio κ_c/κ_b between the conductivities measured for heat currents directed along the c and b axes, respectively, comparing the data of Lussier *et al.*[7] to weak-coupling BCS calculations using order-parameters representative of the E_{1g} and E_{2u} symmetry classes of the D_{6h} space group of the hexagonal crystal. While both states have lines of order-parameter nodes (and hence higher density of excited quasiparticles) in the basal plane, the E_{2u} state has point nodes along the c axis where the order parameter vanishes quadratically, in contrast to the linear behavior in the E_{1g} state. In consequence, the thermal conductivity (and indeed all current-current correlation functions) was found to be isotropic in the E_{2u} state over a spherical Fermi-surface, despite the intrinsic anisotropy of the superconducting state. Ellipsoidal Fermi surfaces do not change the value of the normalized conductivity ratio $(\kappa_c/\kappa_{Nc})/(\kappa_b/\kappa_{Nb})$ from unity in this state (N refers to the normal state),[9] but it is clear that the true hexagonal crystal structure will do so. Furthermore, is not clear whether this result is specific to the particular E_{2u} state analyzed, or would hold for a more general E_{2u} state. Understanding the extent to which these factors might improve the agreement with the large measured anisotropy is crucial to the E_{2u} scenario proposed by Sauls and Norman[2] in which several problems characteristic of GL theories of type (i) above are resolved.

In this paper, we study the influence of both Fermi surface anisotropy and gap anisotropy on superconducting state transport coefficients, focusing on the thermal conductivity data of Lussier *et al.*[7,10] In the first part, we use a simple ellipsoidal Fermi surface fit to normal-state transport data and analyze all gap functions represented by ellipsoidal harmonics up through $L=5$, treating various impurity scattering rates, impurity phase shifts, and inelastic-scattering effects. First, we find that a finite, nonzero $T=0$ value of the thermal conductivity ratio, $\kappa_c(0)/\kappa_b(0)$, of intrinsic origin occurs

for a number of harmonics, not just those of E_{2u} symmetry. Second, we find that the data can be fit reasonably well by gaps of both E_{1g} and E_{2u} symmetry, with the latter fitting slightly better than the former, although in neither case is a pure harmonic realized. These fits could be differentiated more clearly by (1) extending the measurements to lower temperatures or (2) by increasing or decreasing the impurity scattering rate, that is, by analyzing cleaner or dirtier samples. Although fits using ellipsoidal harmonics may be somewhat unrealistic, they allow us to obtain some useful analytical results, and determine the qualitative features of order parameter anisotropy with some confidence.

In the second part, we turn to the more general case, using the multisheeted Fermi surface predicted from local-density approximation (LDA) calculations[11] which is in reasonable agreement with de Haas–van Alphen (dHvA) experiments,[12] up to an overall mass renormalization. Two types of gap functions are analyzed: Fermi-surface harmonic[13] and tight binding.[14,15] In neither case is an adequate fit found to the data for either E_{2u} or E_{1g} with single basis functions, although one of the tight-binding gap functions of E_{1g} symmetry has some promise. In the Fermi-surface harmonic case, this poor agreement is due to the large number of nodes these functions possess which is unlikely to arise out of any microscopic gap equation. In the tight-binding case, this is likely due to the use of a single basis function. Use of a mixed basis set in the tight-binding case leads to a good correspondence to the data in the E_{1g} case. So far, we have not found a comparably good fit for the E_{2u} case.

I. ORDER PARAMETERS AND FERMI SURFACES

Although a variety of models have been proposed for the order parameter of UPt_3, we concentrate here on the most popular model, that of a two-dimensional group representation. The two variants most commonly explored have been the E_{1g} model[16] and the E_{2u} model.[2] For a spherical Fermi surface, the gap function can be represented by spherical harmonics. A function of E_{1g} symmetry first occurs in the $L=2$, $M=1$ representation (d wave). The E_{2u} case is more subtle since it is an odd-parity gap and therefore a pseudospin triplet.[17] The proposed E_{2u} model assumes that the gap is a pure spin triplet with only one component ($S_z=0$) condensed, however. In this case, E_{2u} first occurs for Y_{32} (f wave). The E_{2u} model based on Y_{32} was originally proposed[18] since (i) its nodal structure was similar to the previously considered E_{1g} model based on Y_{21}, with line nodes perpendicular to the c axis and point nodes along the c axis as indicated by transverse ultrasound[1] as well as point contact spectroscopy,[19] and (ii) it has an upper critical field anisotropy consistent with experimental data[20] given the $S_z=0$ orientation of the triplet order parameter, as demonstrated earlier by Choi and Sauls[21] (singlet order parameters give an incorrect anisotropy). Sauls[2] in turn showed that this model solved a major problem of the previously considered E_{1g} model, in that it could explain the existence of a tetracritical point in the H-T phase diagram for all orientations of the magnetic field as observed experimentally, at least for axial symmetry. Recently, Park and Joynt[22] have proposed that E_{1g} can avoid the problem of an incorrect upper critical field anisotropy if the normal-state Pauli susceptibility has opposite anisotropy to the observed normal-state susceptibility (the latter likely being van Vleck dominated). It can also give a phase diagram which has a near tetracritical point for certain choices of the GL coefficients, with the additional claim that it gives a better explanation of the pressure-temperature phase diagram than E_{2u}.

A potential method of resolving these controversies would be to obtain more knowledge of the actual form of the gap anisotropy. The E_{1g} model has a linear dispersion of the quasiparticle energies about the point nodes, whereas the E_{2u} model has a quadratic dispersion. This can have a significant effect on transport quantities, as pointed out by Yin and Maki.[23] Fledderjohann and Hirschfeld[8] exploited this to show that the thermal conductivity anisotropy ratio, $\kappa_c(0)/\kappa_b(0)$, is small for the E_{1g} case (it would be zero in the clean limit), but is unity for the E_{2u} case, at least for an ellipsoidal Fermi surface, with the data of Lussier *et al.*[7] lying between these two results but being more consistent with E_{1g} than E_{2u}. This in turn motivated Lussier *et al.* to take data at lower temperatures, where they conclude that the extrapolated $T=0$ anisotropy ratio of about 0.5 is probably intrinsic and thus consistent with an E_{2u} model.[10]

The above analysis of Fledderjohann and Hirschfeld[8] was based on a particular spherical harmonic form of the order parameter on an ellipsoidal Fermi surface. For a real metal like UPt_3, we would expect that the actual order parameter is more complicated, just as we know that the actual Fermi surface is multisheeted and shows strong deviations from axial symmetry.[12] The latter is particularly important since the E_{2u} result $\kappa_c/\kappa_b=1$ is a consequence of axial symmetry.

To analyze this in more detail, we first consider the simple ellipsoidal case treated previously, but look at other harmonics besides Y_{21} and Y_{32}. The conversion from spherical to ellipsoidal harmonics can be achieved by replacing $\sin(\theta)$ by $\sin(\theta)/\sqrt{m_r}$ and r^2 (previously unity) by $\cos^2(\theta)+\sin^2(\theta)/m_r$,[24] where the mass ratio, $m_r=m_\perp/m_c$, is equal to 2.8 based on normal-state transport data.[7] Note that this conversion simply multiplies Y_{21} and Y_{32} by an overall constant, so the results for these two cases are independent of the mass ratio. This is not true in general. For the E_{1g} case, the next higher harmonic to consider is Y_{41}; for the E_{2u} case ($S_z=0$), Y_{52}. Although such higher harmonics seem exotic, they do play a significant role in certain microscopic theories.[25]

For the real Fermi-surface case, we utilize the surface obtained from an LDA calculation.[11,26] This surface, which is shown in symmetry planes of the zone in Fig. 1, is in reasonable agreement with dHvA data, except for mass renormalization effects. The mass renormalization would play no role here unless it was anisotropic. Unfortunately, there is not enough data available to model this anisotropy, although the lack of observation of dHvA orbits for fields along the c axis suggests that the renormalization is anisotropic and will act to increase the mass ratio, m_r.[12] To check this, we calculated $\langle v_c^2\rangle/\langle v_b^2\rangle$ where v_b and v_c are the Fermi velocities and $\langle\ \rangle$ is an average over the Fermi surface determined by using a linear tetrahedron decomposition of the Brillouin zone.[27,28] This quantity, equal to the ratio κ_{Nc}/κ_{Nb} given the observation of isotropic relaxation time,[7] is 2.8 from thermal conductivity and 2.7 from resistivity.[7] The LDA calculation

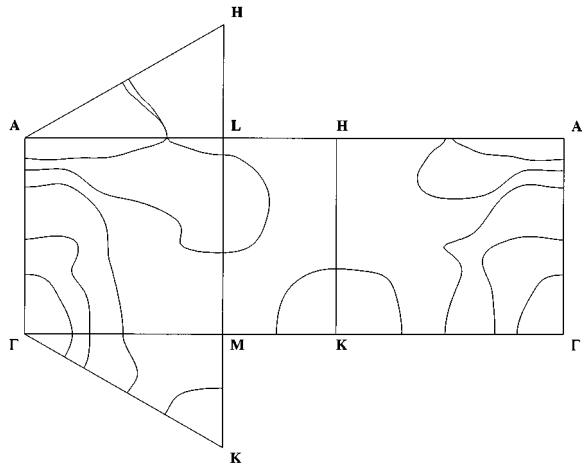

FIG. 1. LDA Fermi surface for UPt_3 plotted in the symmetry planes of the Brillouin zone. The surface is composed of five bands, three centered around Γ and two centered around A.

gives 2.1. This is consistent with the above observation that the mass renormalization anisotropy acts to increase m_r. Since we are comparing in this paper to data normalized to the normal-state value, we ignore this mass ratio discrepancy in this paper, although we caution that it could influence some of the results presented here. In particular, an alteration in Fermi-surface topology would certainly change the gap anisotropy, but even a momentum dependence of the mass renormalization would affect the results since this would act to alter the weighting of various momentum vectors in the equations.

The problem of what gap function to use for the real Fermi surface case is a more complicated issue. Allen showed a number of years ago that functions could be constructed on the Fermi surface which were orthornormal and so could be used as basis functions, which he labeled Fermi-surface harmonics.[13] They can be obtained from the spherical harmonics by replacing k_i by v_i,[24] although there are more Fermi-surface harmonics for a given power of v_i than there are spherical harmonics since the lattice symmetry is discrete rather than continuous. A complication is that the relative size of the gap function on independent sheets of the Fermi surface cannot be determined outside the context of a microscopic theory of the superconductivity. In fact, the problem is a more general one since the simple gap functions treated here are likely to be modulated at each k vector by some complicated function (of A_{1g} symmetry) that contains the affects of wave function anisotropy, etc. We further note that the Fermi-surface harmonics will be small when the Fermi velocities are small. On the other hand, we would anticipate that in most microscopic theories, the gap function will be large where the f electron weight is highest, which is also where the Fermi velocities will in general be lowest. Keeping these caveats in mind, we define Fermi-surface harmonics for the E_{1g} case and E_{2u} case by replacing k_i by v_i in the Y_{21} and Y_{32} spherical harmonics. That is, the modulus of the E_{1g} gap is $v_c v_r$ and the E_{2u} gap $v_c v_r^2$ where $v_r^2 = v_a^2 + v_b^2$.[29] The nodal structure of these functions are very complicated given the complicated Fermi-surface geometry. There are many points on the Fermi surface where the velocity vector points either along or perpendicular to the c axis. In any of these cases, the E_{1g} and E_{2u} Fermi-surface harmonics will vanish.

An alternate set of basis functions can be generated by tight-binding expansion. In the square lattice case, the lattice vectors of type (1,0) lead to a d-wave state of the form $\cos(k_x)-\cos(k_y)$, which is currently the leading model being explored for high-temperature cuprates. For the hexagonal closed-packed case, E_{1g} and E_{2u} first appear for primitive lattice vectors of the type (0,1,1). These can be generated from the next-near-neighbor basis functions listed by Putikka and Joynt[14] by multiplying their E_{1u} and E_{2g} functions by $\sin(k_z c)$. They are for E_{1g}

$$f_1 = \sqrt{2}\,\sin(k_z c)\cos\left(\frac{1}{2}k_y a\right)\sin\left(\frac{\sqrt{3}}{2}k_x a\right),$$

$$f_2 = \frac{2}{\sqrt{6}}\sin(k_z c)\left[\sin(k_y a)+\sin\left(\frac{1}{2}k_y a\right)\cos\left(\frac{\sqrt{3}}{2}k_x a\right)\right], \tag{1}$$

and for E_{2u}

$$f_1 = \frac{2}{\sqrt{6}}\sin(k_z c)\left[\cos(k_y a)-\cos\left(\frac{1}{2}k_y a\right)\cos\left(\frac{\sqrt{3}}{2}k_x a\right)\right],$$

$$f_2 = \sqrt{2}\,\sin(k_z c)\sin\left(\frac{1}{2}k_y a\right)\sin\left(\frac{\sqrt{3}}{2}k_x a\right), \tag{2}$$

with a gap modulus of $\sqrt{f_1^2+f_2^2}$ for an assumed gap of the form f_1+if_2 (the 1,i state). Both functions have line nodes in the $k_z=0$ and $k_z=\pi/c$ planes. In addition, the E_{1g} function has point nodes with linear dispersion along all three symmetry axes ($\Gamma-A$, $M-L$, $K-H$), whereas E_{2u} has quadratic point nodes along $\Gamma-A$ and linear point nodes along $K-H$. We note that the basis functions listed by Putikka and Joynt for the near-neighbor case are not properly invariant under reciprocal-lattice translations due to the nonsymmorphic nature of the UPt_3 lattice (that is, the near neighbors are separated by a nonprimitive translation vector). This problem has been addressed by Konno and Ueda.[15] Under the highly simplistic assumption that the phase of the single-particle wave functions on the two sites in the unit cell is determined by a simple near-neighbor interaction, they were able to generate analytic near neighbor basis functions which have proper translational symmetry. In this paper, we use their Γ_6^+ (E_{1g}) and Γ_5^- (E_{2u}) basis functions. These, in fact, can be generated from the tight-binding basis functions discussed above by replacing $\sin(k_z c)$ by $\sin(k_z c/2)/|\phi|$ where ϕ is the Fourier transform of the near-neighbor distance vectors projected onto the basal plane

$$\phi = \frac{1}{\sqrt{3}}\left[e^{i(k_x a/\sqrt{3})}+2\,\cos\left(\frac{k_y a}{2}\right)e^{-i(k_x a/2\sqrt{3})}\right] \tag{3}$$

(ϕ is complex since the lattice is nonsymmorphic). The effect of this is to remove the line nodes in the $k_z=\pi/c$ plane and the linear point nodes along $K-H$.

II. THERMAL CONDUCTIVITY

The thermal conductivity κ in the presence of impurities is evaluated using a Kubo formula for the heat-current correlation function as in the original treatment for an s-wave superconductor by Ambegaokar and Tewordt.[30] This treatment was generalized to unconventional states by several groups, giving results for a spherical Fermi surface and model p- and d-wave states which agreed qualitatively with experiment.[4,5,31,32] In the limit of vanishing impurity concentrations, identical results were also obtained by Arfi *et al.*[33] using a transport equation method.

The Kubo formula approach begins with an impurity-averaged single-particle matrix propagator

$$\underline{g}(\mathbf{k},\omega)=\frac{\tilde{\omega}\underline{\tau}^0+\xi_{\mathbf{k}}\underline{\tau}^3+\underline{\Delta}_{\mathbf{k}}}{\tilde{\omega}^2-\xi_{\mathbf{k}}^2-|\Delta_{\mathbf{k}}|^2}, \tag{4}$$

where $\underline{\tau}^i$ represent the Pauli matrices spanning particle-hole space. Here, we have already exploited the approximate particle-hole symmetry of the normal state, as well as the symmetries of the gap functions which lead to vanishing off-diagonal scattering self-energy contributions. In this limit, only self-energy contibutions to the frequency ω, namely $\tilde{\omega}=\omega-\Sigma_0$ need to be included.[32] The self-energy Σ_0 due to the elastic impurity scattering is treated in a self-consistent T-matrix approximation and is given by $\Sigma_0=\Gamma G_0/(c^2-G_0^2)$, where $\Gamma=n_i n/(\pi N_0)$ is the unitarity limit scattering rate depending on the concentration of defects n_i, the electron density n, and the density of states at the Fermi level N_0. The quantity $c\equiv\cot\delta_0$ parametrizes the scattering strength of an individual impurity through the s wave phase shift δ_0. In this work we consider primarily unitarity limit scattering $c=0$, since it is clear that weak scattering will lead to a weak temperature dependence inconsistent with experiment for the states in question.[34,35] The integrated propagator is $G_0=(1/2\pi N_0)\Sigma_{\mathbf{k}}\mathrm{Tr}\{\underline{\tau}^0\underline{g}(\mathbf{k},\omega)\}$. The equation for the self-energies are now solved self-consistently. We ignore the complication of resolving the gap equation in this paper since all results are scaled to T_c and impurity corrections are small. The gap itself is given by

$$\Delta_{\vec{k}}(T)=\Delta_{\mathrm{BCS}}(T)e^{-\langle f_{\vec{k}}^2\ln|f_{\vec{k}}|\rangle/\langle f_{\vec{k}}^2\rangle}f_{\vec{k}}, \tag{5}$$

where $\Delta_{\mathrm{BCS}}(T)$ is the BCS gap and $f_{\vec{k}}$ is one of the basis functions (or mixtures thereof) described in the previous section.

The bare heat current response is given by a convolution of the Green's function g with itself at zero external frequency and wave vector weighted with the bare heat current vertex $\omega\mathbf{v}_{\mathbf{k}}\underline{\tau}^3$.[30] Impurity scattering vertex corrections to current-current correlation functions have been shown to vanish identically for even parity states ($\Delta_{\mathbf{k}}=\Delta_{-\mathbf{k}}$).[32] Even for odd-parity states, such corrections vanish in the unitarity limit. For the diagonal thermal conductivity tensor one obtains

$$\frac{\kappa_i(T)/T}{\kappa_{N,i}(T_c)/T_c}=\frac{3\Gamma_N}{4\pi^2}\int_0^\infty\frac{d\omega}{T}\left(\frac{\omega}{T}\right)^2\mathrm{sech}^2\left(\frac{\omega}{2T}\right)K_i(\omega,T), \tag{6}$$

$$K_i(\omega,T)=\frac{1}{\tilde{\omega}'\tilde{\omega}''}\mathrm{Re}\int\frac{dS_{\mathbf{k}}}{|\mathbf{v}_{\mathbf{k}}|}\frac{\mathbf{v}_{\mathbf{k}i}^2}{\langle\mathbf{v}_{\mathbf{k}i}^2\rangle}\frac{\tilde{\omega}^2+|\tilde{\omega}|^2-2|\Delta_{\mathbf{k}}|^2}{\sqrt{\tilde{\omega}^2-|\Delta_{\mathbf{k}}|^2}}, \tag{7}$$

where $\tilde{\omega}'$ and $\tilde{\omega}''$ are the real and imaginary parts of $\tilde{\omega}$ and $\Gamma_N\equiv\Gamma/(1+c^2)$ is the normal-state scattering rate. Here $dS_{\mathbf{k}}$ is the area measure on the Fermi surface, and $v_{\mathbf{k}}$ is the Fermi velocity.

For a complete description of the data, we must take into account the effects of inelastic scattering. This is known to vary as bT^2 times the elastic rate in the normal state, with $b\simeq 4/K^2$.[7] This effect can be included in the above equations by replacing Γ by $\Gamma(1+bT^2)$. In the superconducting state, we can make the ansatz that the inelastic rate varies as bT^3/T_c since the number of quasiparticles varies as T/T_c at low temperatures due to the line nodes in the gap.[36] The exact form of this makes little difference, since by far the largest effect inelastic scattering has is on $\kappa_N(T)$. Therefore, for practical purposes when comparing to data normalized to its value at T_c, one can simply scale the result of Eq. (6) by $(1+bT_c^2)/(1+bT^2)$.

Finally, we note that UPt_3 has a split superconducting phase transition. In the E models considered here, this splitting is assumed to be due to the weak antiferromagnetism which has orthorhombic symmetry. Its effect is to cause only one of the two E components to condense at the upper phase transition. Thus, in the region between the upper ($T_{c+}=0.50$ K) and lower ($T_{c-}=0.44$ K) transitions, the point nodes along the c axis become line nodes perpendicular to the basal plane. This explains the lack of gap anisotropy in the thermal conductivity observed in this region. Below T_{c-}, the second E component condenses, and the anisotropy begins to occur, as observed. Modeling this is complicated since the calculation would have to be performed for orthorhombic symmetry with two different gaps and appropriate domain averaging performed. We therefore take the approach of previous work which ignores this symmetry breaking but normalizes κ_c/κ_b to its value at T_{c-}.[7,8,10] This normalization does not work so well, though, when comparing to the individual $\kappa_i(T)/T$ themselves, since the thermal conductivity does change above T_{c-}. We have found that normalizing $\kappa_i(T)/T$ to its value at $T_{c0}=0.47$ K, the average of T_{c+} and T_{c-} (the "hexagonal" T_c), works quite well in this regard. Obviously, one cannot take too seriously the results in the immediate vicinity of T_c until the effects of the symmetry-breaking field are properly included.

III. RESULTS

A. Ellipsoidal harmonics

Results for κ_c/κ_b are shown in Fig. 2 for all harmonics through $L=5$ on an ellipsoidal Fermi surface with $m_r=2.8$, compared to the experimental results of Lussier *et al.*[10] This quantity is normalized to its value at T_{c-} as discussed above. The results were generated with an impurity scattering rate in the unitarity limit of $0.1T_c$, consistent with experimental data (particularly with the observation of a residual linear specific-heat coefficient of 0.16 the normal-state value).[10] To understand these results more clearly, we have analytically calculated

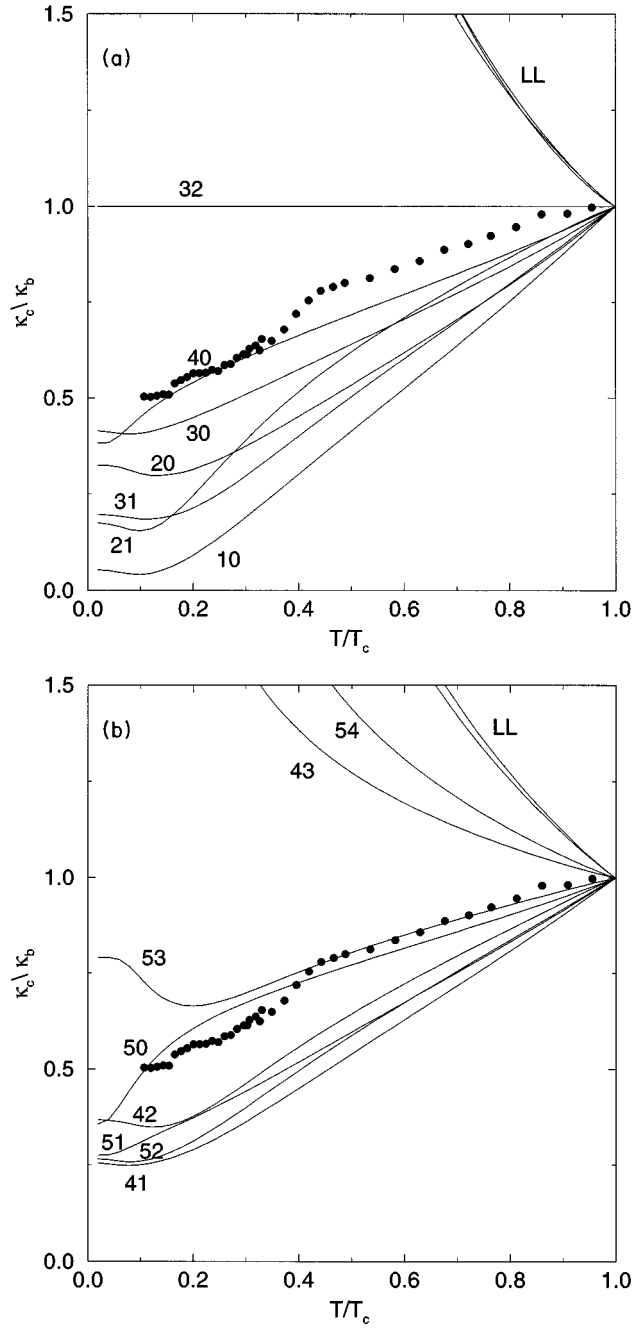

FIG. 2. κ_c/κ_b (normalized to its value at T_{c-}) for various harmonics through $L=5$ (curves labled by L,M) on an ellipsoid ($m_r=2.8$). All plots, unless otherwise noted, are for an impurity scattering rate Γ of $0.1T_c$ in the unitarity limit, with an inelastic-scattering rate $4T^2$ times the elastic rate. The black dots are data from Ref. 10.

$$\frac{\kappa_c(0)}{\kappa_b(0)} = \lim_{\omega\to 0} \frac{\mathrm{Re}\langle v_c^2\sqrt{\omega^2-\Delta_k^2}\rangle}{\mathrm{Re}\langle v_b^2\sqrt{\omega^2-\Delta_k^2}\rangle}\,. \tag{8}$$

In the clean limit for a spherical Fermi surface, and show these results in Table I. We see that harmonics of the form Y_{LL}, which have only point nodes along the c axis, give a divergent ratio. On the other hand, only two of the remaining harmonics, Y_{10} and Y_{21}, give a ratio of zero [the nonzero value in Fig. 2(a) is due to impurity-induced gaplessness[8]],

TABLE I. $\kappa_c(0)/\kappa_b(0)$ in the clean limit for several Y_{LM} gap functions for two values of the mass ratio, m_r. The harmonics Y_{21} and Y_{41} have E_{1g} symmetry and the harmonics Y_{32}, Y_{52}, and Y_{54} have E_{2u} symmetry.

LM	Form	$m_r=1$	$m_r=2.8$
10	$\cos(\theta)$	0	0
11	$\sin(\theta)$	∞	∞
20	$3\cos^2(\theta)-r^2$	1	0.357
21	$\sin(\theta)\cos(\theta)$	0	0
22	$\sin^2(\theta)$	∞	∞
30	$\cos(\theta)[5\cos^2(\theta)-3r^2]$	6/7	0.423
31	$\sin(\theta)[5\cos^2(\theta)-r^2]$	1/2	0.180
32	$\sin^2(\theta)\cos(\theta)$	1	1
33	$\sin^3(\theta)$	∞	∞
41	$\sin(\theta)[7\cos^3(\theta)-3\cos(\theta)r^2]$	0.647	0.252
52	$\sin^2(\theta)[3\cos^3(\theta)-\cos(\theta)r^2]$	0.744	0.267
54	$\sin^4(\theta)\cos(\theta)$	∞	∞

with the rest giving an intrinsic nonzero ratio. In particular, we note that harmonics of the form Y_{L0} only have line nodes, so a finite, nonzero ratio is not something just associated with quadratic point nodes or with gaps of E_{2u} symmetry. We also note that no pure harmonic provides a good fit to the observed anisotropy,[24] although some higher harmonics give adequate fits.

To study this further, we have looked into the possibility of mixed solutions. For E_{1g}, we included mixing of Y_{21} with Y_{41}; for E_{2u}, Y_{32} with Y_{52}.[37] Typical results for κ_c/κ_b are shown in Fig. 3(a), with the coefficients roughly optimized to fit the data. Both fits give a reasonable description of the data, with the lowest temperature data intermediate between the two results (it should be remarked that the error bars on the experimental κ_c/κ_b are about 15% at low temperature[10]). The E_{1g} fit can be greatly improved at lower temperature by going to a larger scattering rate of $0.3\,T_c$, but the individual κ_i/T in this case are in poor agreement with experiment. Altering the scattering phase shift from the unitarity value of $\cot(\delta_0)$ of 0 to 0.2 slightly improves things at the lowest temperatures, but this is probably not significant given the experimental error bars. For the E_{2u} case, lowering the scattering rate by a factor of 10 only slightly suppresses the ratio and only for temperatures below where experimental data exist [the same slight suppression also occurs by increasing $\cot(\delta_0)$]. In Fig. 3(b), we compare these fits to the individual κ_i/T, normalized to their value at T_{c0} as discussed previously. As can be seen, both E_{1g} and E_{2u} provide good fits to the data, with the E_{2u} fit being slightly superior. An interesting point is that the experimental κ_i/T are linear in temperature down to the lowest measured temperatures. This behavior cannot continue indefinitely since κ_i/T would be zero at a temperature larger than zero (that is, κ_i/T must flatten off). The calculated curves, though, predict that this flattening should occur in the measured temperature range in contradiction with experiment. As suggested by the authors of Ref. 10, the calculated low-temperature behavior can be improved by reducing Γ to roughly one-tenth its normal-state value. Although this does improve the fit at low temperatures, it leads to a substantial deviation from the data at higher tem-

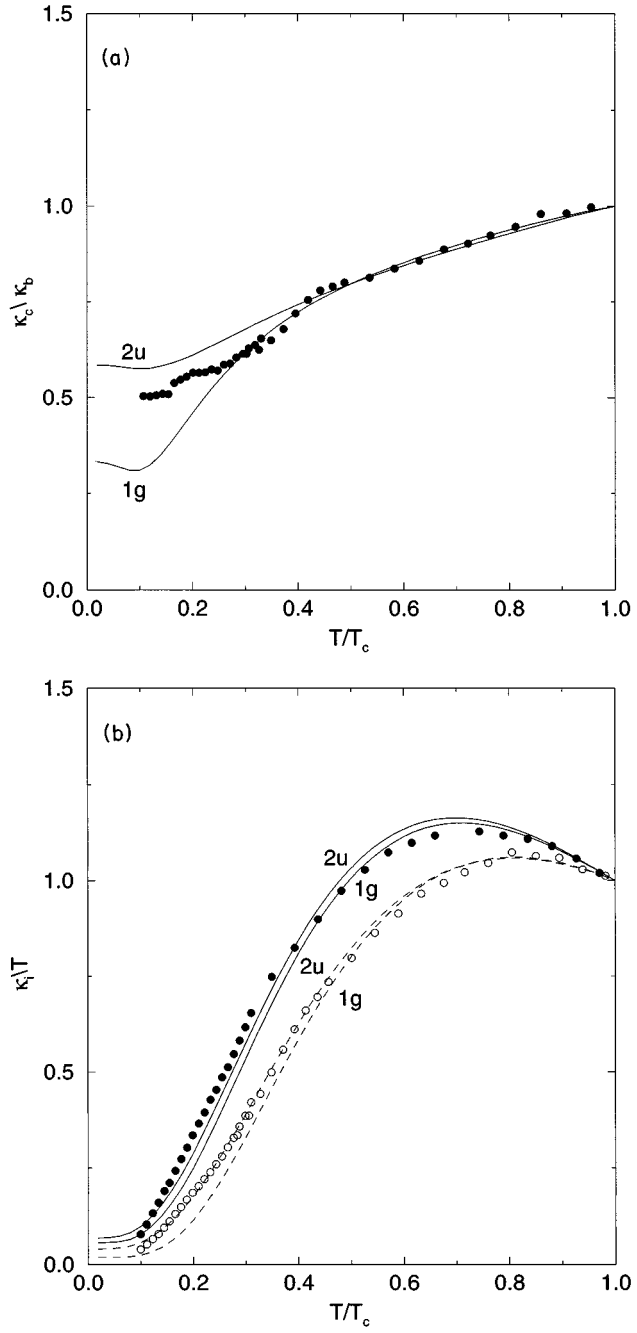

FIG. 3. (a) κ_c/κ_b and (b) κ_i/T for mixed harmonics on an ellipsoid ($m_r=2.8$). The curve marked $1g$ is for E_{1g} ($Y_{21}-0.15Y_{41}$) and the one marked $2u$ for E_{2u} ($Y_{32}+0.2Y_{52}$). Black dots in (a) and black (white) dots in (b) are data from Ref. 10. The solid (dashed) curves in (b) are the respective theoretical results for $i=b$ ($i=c$).

peratures. In fact, we have found that the value $\Gamma/T_c\sim 0.1$ (the normal-state value) gives roughly the best fit over the entire temperature range below T_c. We have also found that altering the scattering phase shift from the unitarity value of $\pi/2$ does not improve the fit in this regard, at least for small values of $\cot(\delta_0)$. If this discrepancy between the low-temperature and high-temperature behavior is taken at face value, a strong temperature dependence of either $c=\cot(\delta_0)$ or Γ must be assumed. Although dynamical scattering effects could easily influence the phase shifts in this way, we have

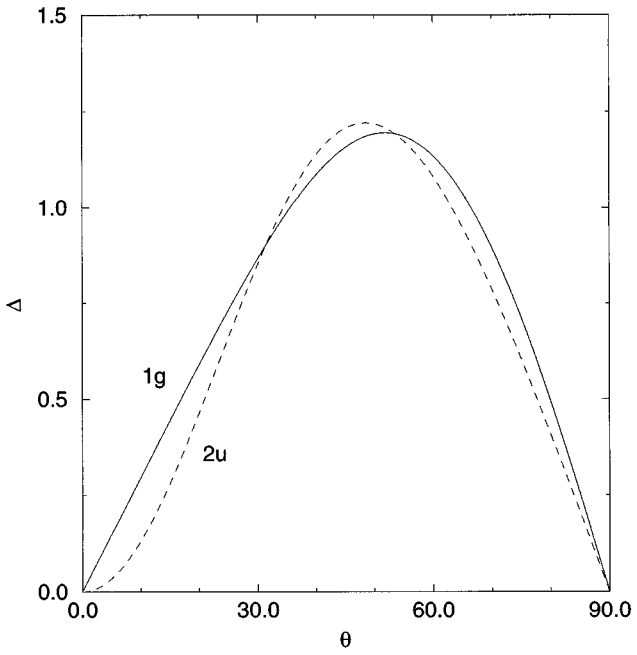

FIG. 4. Order parameter versus polar angle for mixed harmonics on an ellipsoid ($m_r=2.8$).

been unable to find a satisfactory phenomenological explanation of the data in these terms. While a T-dependent parametrization of Γ could possibly account for the discrepancy, we have no physical understanding of how such effects could arise.

The gap functions in the E_{1g} and E_{2u} cases are plotted as a function of polar angle in Fig. 4. Both gap functions look similar (except for the different dispersions around the point

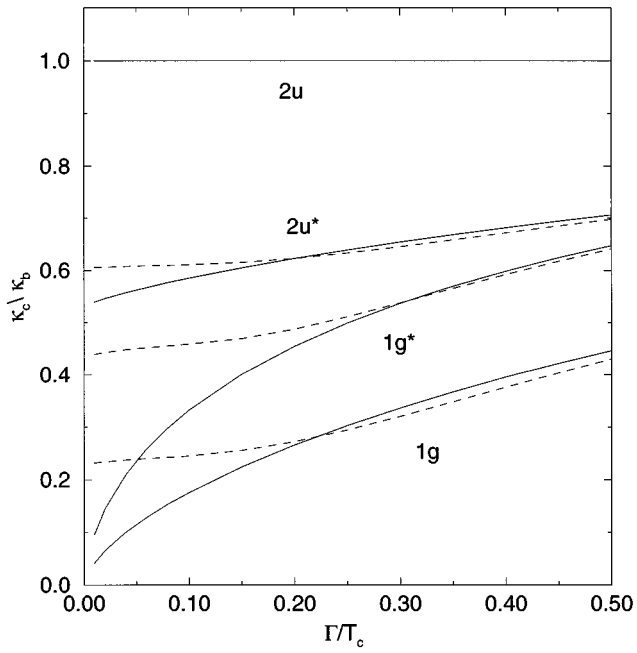

FIG. 5. κ_c/κ_b at $T/T_c=0.02$ (solid line) and $T/T_c=0.2$ (dashed line) vs normalized impurity scattering rate, Γ/T_c, for pure ellipsoidal harmonics Y_{32} ($2u$) and Y_{21} ($1g$), as well as for the mixed harmonics of Fig. 3(a) ($2u^*$ and $1g^*$).

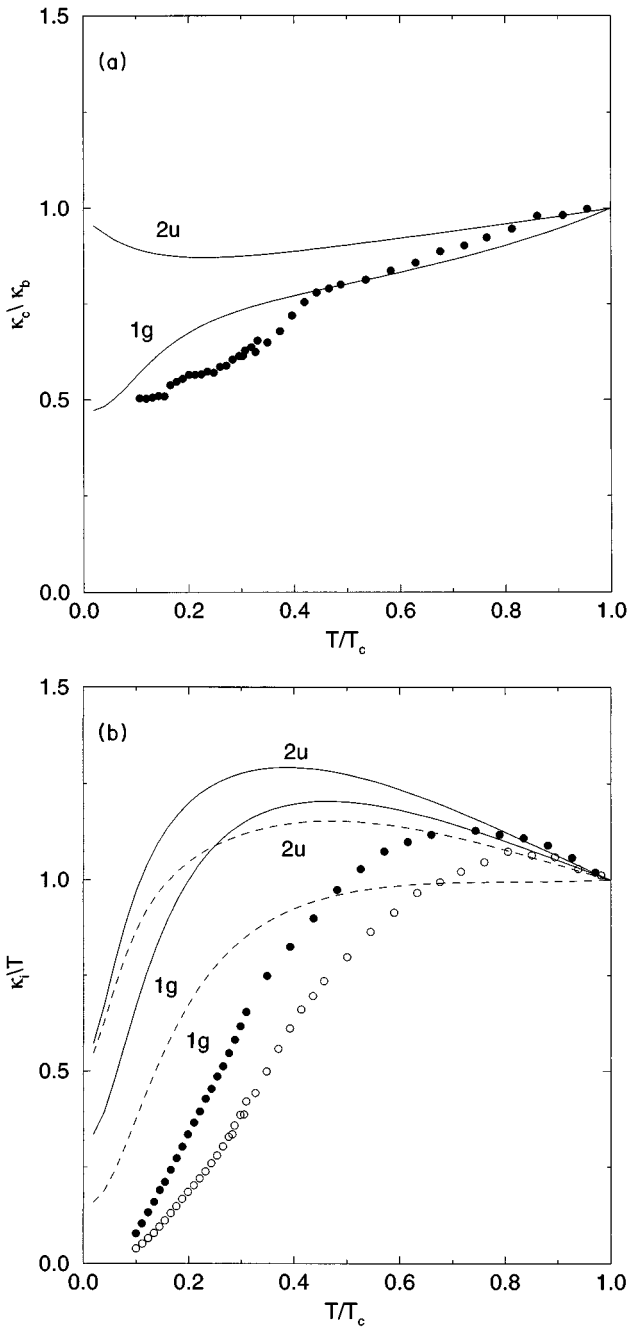

FIG. 6. (a) κ_c/κ_b and (b) κ_i/T for Fermi-surface harmonics on the LDA Fermi surface. Same notation as Fig. 3.

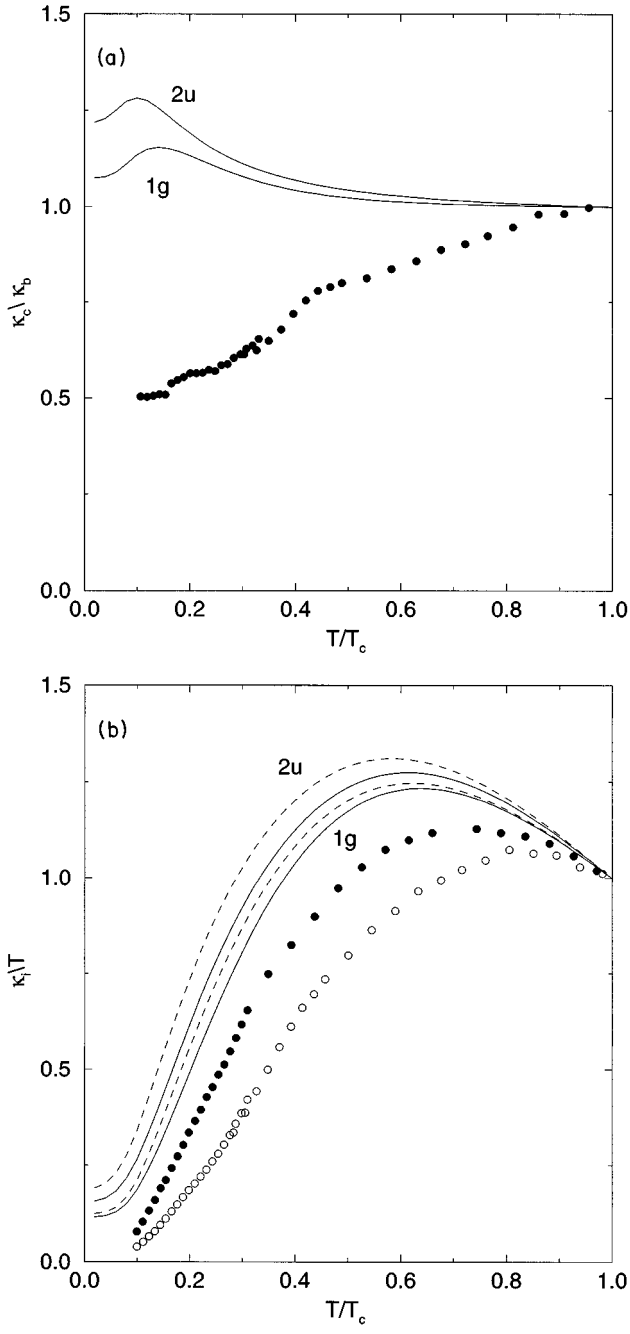

FIG. 7. (a) κ_c/κ_b and (b) κ_i/T for tight-binding functions (0,1,1 type primitive lattice vectors) on the LDA Fermi surface. Same notation as Fig. 3.

nodes at zero degrees). This indicates that the primary determinant of the thermal conductivity is the overall shape of the gap function. We also note that the maximum gap occurs at a polar angle of 52° for E_{1g} and 49° for E_{2u}. Not only are these angles close, but they are also close to the angle of 54° that the vector connecting near neighbor uranium atoms makes with the c axis. This could be taken as indirect evidence that the electrons in the Cooper pairs reside at near-neighbor sites as would be predicted by microscopic models based on antiferromagnetic spin fluctuations.

We conclude this part by remarking that both the E_{1g} and E_{2u} models can explain the data. One way to more clearly distinguish between the two would be to carry the experiments to lower temperatures, although given experimental error bars, it may be difficult to conclude anything definitive. At the least, one would hope to see κ_i/T flatten off. Perhaps a better way would be to degrade the quality of the sample. In the presence of a finite concentration of impurities, states with line nodes yield a linear term in the thermal conductivity, $\kappa_i(T) \sim T/\Delta_0$ at the lowest temperatures. For generic configurations of the thermal current $\mathbf{j}_Q$ and the line nodes, the proportionality constant is actually independent of the impurity scattering rate to leading order, yielding a universal value for the low-T thermal conductivity analogous to the electrical conductivity result found by Lee.[38] In the final

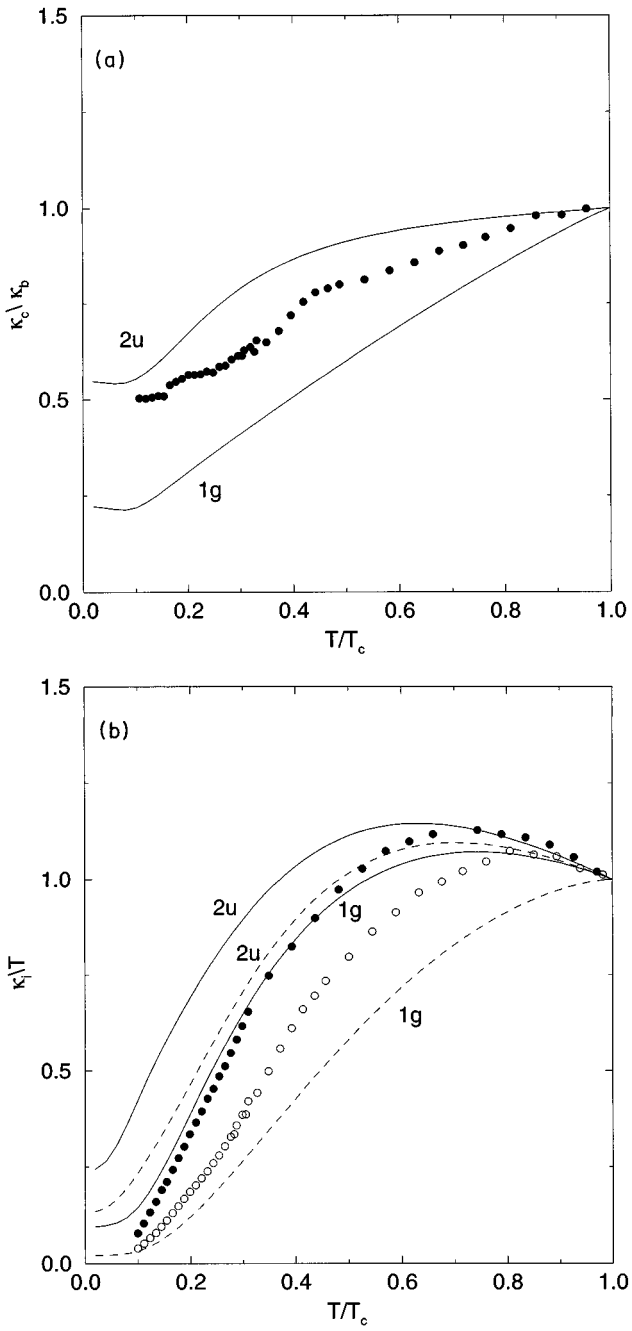

FIG. 8. (a) κ_c/κ_b and (b) κ_i/T for near-neighbor tight-binding functions (Konno-Ueda type) on the LDA Fermi surface. Same notation as Fig. 3.

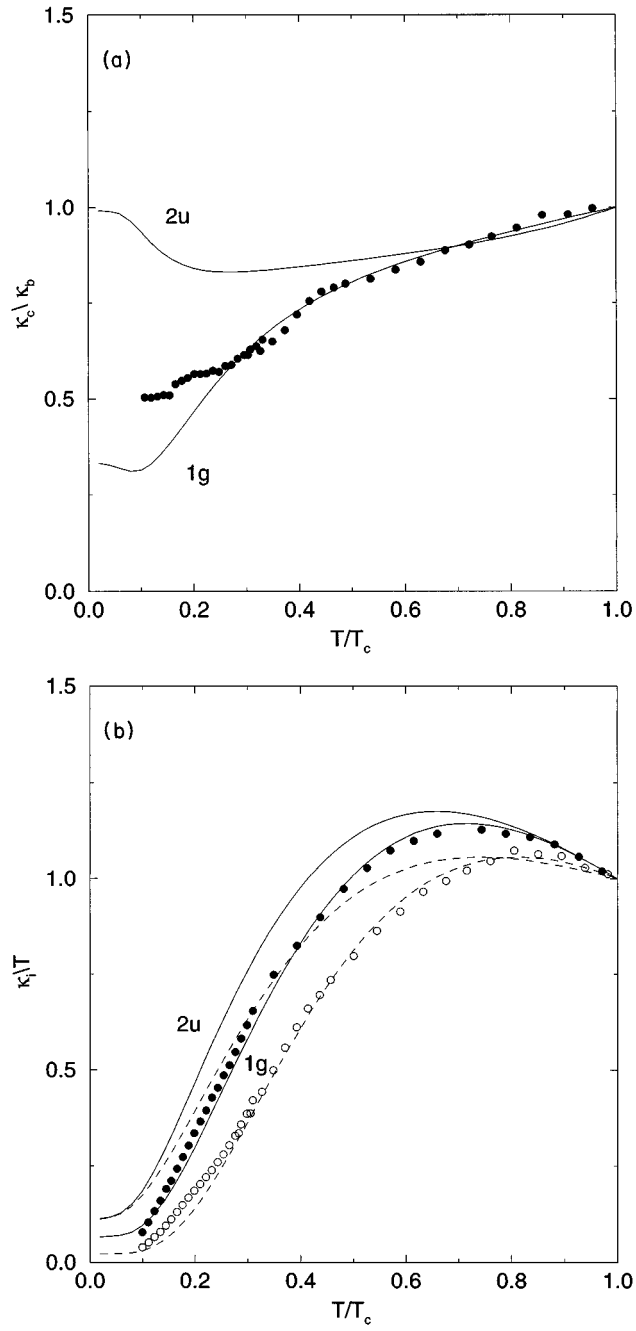

FIG. 9. (a) κ_c/κ_b and (b) κ_i/T for mixed tight-binding functions on the LDA Fermi surface. Same notation as Fig. 3.

stages of writing, we received a paper from Graf *et al.*[39] in which this result was obtained independently and explored in some detail.

Because of impurity-induced gapless effects of this type, the anisotropy ratio $\kappa_c(0)/\kappa_b(0)$ is always finite even for states like E_{1g}, as mentioned above. In such a situation, an estimate of the anisotropy may be performed by considering Eq. (7) in the gapless regime, i.e., take $\tilde{\omega}=a\omega+i\gamma$, with a, γ constant. We then find $\kappa_c(0)/\kappa_b(0)=\langle v_c^2F_k^3\rangle/\langle v_b^2F_k^3\rangle$, with $F_k=(\gamma^2+\Delta_k^2)^{-1/2}$. For the Y_{21} case (E_{1g}) in spherical symmetry, we find $\kappa_b(T)\sim T/\Delta_0$, $\kappa_c(T)\sim\gamma T/\Delta_0^2$, giving $\kappa_c(0)/\kappa_b(0)\simeq 2\gamma/\Delta_0$ for small concentrations. The residual broadening γ is found by solving the transcendental equation $c^2+\gamma^2\langle F_k\rangle^2=\Gamma\langle F_k\rangle$, and yields a square-root dependence on concentration, $\kappa_c(0)/\kappa_b(0)\sim(\Gamma/\Delta_0)^{1/2}$ up to logarithmic corrections in the unitarity limit $c=0$. In Fig. 5, we plot the impurity concentration dependence of the anisotropy ratio in both E_{1g} and E_{2u} cases for $T=0.02$ and $0.2T_c$. We note the qualitatively stronger dependence of the anisotropy ratio on impurity scattering rate for the E_{1g} case as compared to the E_{2u} case at low temperatures.

B. Fermi-surface harmonics

The above analysis assumes an ellipsoidal Fermi surface. The actual Fermi surface for UPt_3 is very complicated and

could substantially alter the above conclusions. In this part, we present results using Fermi-surface harmonic gap functions as described in the first section with the Fermi surface shown in Fig. 1. We again assume an impurity scattering rate of $0.1T_c$. Results for κ_c/κ_b are shown in Fig. 6(a) and for κ_i/T in Fig. 6(b). The E_{1g} case gives a fair representation of the anisotropy ratio, especially at higher temperatures. Both cases, though, predict too large κ_i/T at lower temperatures. This occurs since the Fermi-surface harmonic gap functions have a very large number of nodes. These nodes are due to the complicated Fermi surface, which has many points on it where the velocity vector is either parallel or perpendicular to the c axis, either case in which the E_{1g} and E_{2u} Fermi-surface harmonics vanish. This large number of nodes is unlikely to arise out of any microscopic gap equation since such a solution would not have an optimal condensation energy. This indicates that Fermi-surface harmonics are unlikely to be useful in modeling heavy fermion superconductors. Because of this, and since the addition of higher-order harmonics will not reduce the number of nodes, we have not explored using mixed Fermi-surface harmonics as done in the previous subsection for ellipsoidal harmonics.

C. Tight-binding functions

We next present results for tight-binding gap functions. These functions represent short-range interactions in the lattice, and therefore are more likely to arise out of a microscopic gap equation than the Fermi-surface harmonics. Results for the functions based on (0,1,1) type primitive lattice vectors are shown for κ_c/κ_b in Fig. 7(a) and κ_i/T in Fig. 7(b). Although the magnitude of κ_i/T is improved over the Fermi-surface harmonic case, the anisotropy ratio is in poor agreement with experiment. We therefore turn to results using the Konno-Ueda functions based on near-neighbor interactions[15] [Figs. 8(a) and 8(b)]. The observed anisotropy ratio is intermediate between the E_{1g} and E_{2u} cases. Although κ_i/T is too large at lower temperatures for E_{2u}, it is not too bad for E_{1g}. Perfect agreement with experiment would not be expected anyway since the above basis functions do not take into account the complicated single-particle wave functions which occur in heavy fermions due to f orbital degeneracy and f-ligand hybridization. It is interesting to note that the near-neighbor tight-binding functions provide the best overall comparison to the data for those functions we have analyzed on the real Fermi surface, since this reinforces the idea of near-neighbor pairing that was suggested from the ellipsoidal results above. Given this, it will interesting in the future to calculate κ for recent microscopic models which do not involve such pairing.[40]

As in the ellipsoidal harmonic case, to test the idea of whether a mixture of tight-binding basis functions would improve the results, we have done calculations mixing the two tight-binding functions considered above for each symmetry. Only a rough optimization of the mixing coefficients could be determined due to calculational demands. These results are presented in Figs. 9(a) and 9(b). A good fit was obtained for the E_{1g} case with an equal admixture of the two functions. This result is somewhat surprising since an equal admixture would imply (within a tight-binding framework) that the pair interaction has a substantial range [the near-neighbor separation is 7.8 a.u., but an (0,1,1) vector is 14.3 a.u.]. In the E_{2u} case, we never found an adequate fit, although we do show a typical result (equal admixture, but with opposite sign). One should be cautious, though, about ruling against an E_{2u} model based on this, since there are other functions involving nonprimitive translation vectors, with distances comparable to the (0,1,1) primitive vectors, which we have not considered here (one at 13.4 a.u., another at 15.2 a.u.).

IV. CONCLUSIONS

In conclusion, we have found by analyzing simple ellipsoidal models for the Fermi surface that recent thermal conductivity data cannot unambiguously differentiate between the E_{1u} and E_{2u} models for the symmetry of the order parameter. Such a differentiation should be possible by looking at samples with degraded quality, since in the E_{2u} case, the nonzero value of $\kappa_c(0)/\kappa_b(0)$ is intrinsic, whereas for E_{1g}, it is due to impurities. We have also found that results using realistic Fermi surfaces and gaps with proper lattice translational symmetry differ significantly from those based on ellipsoidal Fermi surfaces, and have discovered an E_{1g} tight-binding gap function which gives a good representation of the data. We emphasize that the thermal conductivity data appear to put great constraints on the overall shape of the gap function, and thus will be an important ingredient in determining the validity of microscopic models for the superconductivity in UPt_3.

ACKNOWLEDGMENTS

The authors gratefully acknowledge extensive discussions with L. Taillefer and A. Fledderjohann, and in particular the former for use of his group's unpublished data. M.R.N. was supported by the U.S. Dept. of Energy, Basic Energy Sciences, under Contract No. W-31-109-ENG-38, and also thanks the University of Florida for support in the initial stages of this work.

[1] B. S. Shivaram, Y. H. Jeong, T. F. Rosenbaum, and D. G. Hinks, Phys. Rev. Lett. **56**, 1078 (1986).

[2] For recent reviews, see J. A. Sauls, Adv. Phys. **43**, 113 (1994); L. Taillefer, Hyperfine Interact. **85**, 379 (1994); H. v. Lohneysen, Physica B **197**, 551 (1994); R. H. Heffner and M. R. Norman, Comments Condens. Matter Phys. (to be published).

[3] M. Sigrist and K. Ueda, Rev. Mod. Phys. **63**, 239 (1991).

[4] P. Hirschfeld, D. Vollhardt, and P. Wolfle, Solid State Commun. **59**, 111 (1986).

[5] S. Schmitt-Rink, K. Miyake, and C. M. Varma, Phys. Rev. Lett. **57**, 2575 (1986).

[6] A. Sulpice *et al.*, J. Low Temp. Phys. **62**, 39 (1986).

[7] B. Lussier, B. Ellman, and L. Taillefer, Phys. Rev. Lett. **73**, 3294 (1994).

[8] A. Fledderjohann and P. J. Hirschfeld, Solid State Commun. **94**, 163 (1995).
[9] Some definitions of the harmonics are normalized by the factor r^L, with r no longer a constant in the ellipsoidal case. Inclusion of this normalization increases the E_{2u} value of $\kappa_c(0)/\kappa_b(0)$ by a factor of over 3 for a mass ratio of 2.8. We do not use this normalization factor, since Allen's original paper on Fermi-surface harmonics did not include it (where r would be replaced by the modulus of the Fermi velocity). Still, this ambiguity should be kept in mind.
[10] B. Lussier, B. Ellman, and L. Taillefer, Phys. Rev. B (to be published).
[11] M. R. Norman, R. C. Albers, A. M. Boring, and N. E. Christensen, Solid State Commun. **68**, 245 (1988).
[12] L. Taillefer and G. G. Lonzarich, Phys. Rev. Lett. **60**, 1570 (1988).
[13] P. B. Allen, Phys. Rev. B **13**, 1416 (1976).
[14] W. Putikka and R. Joynt, Phys. Rev. B **37**, 2372 (1988).
[15] R. Konno and K. Ueda, Phys. Rev. B **40**, 4329 (1989).
[16] R. Joynt, J. Magn. Magn. Mater. **108**, 31 (1992).
[17] In the presence of spin orbit, spin is no longer a good quantum number, but one can define a pseudospin since the eigenvalues at a general k point are doubly degenerate due to Kramers theorem.
[18] M. R. Norman, Physica C **194**, 203 (1992).
[19] G. Goll *et al.*, Phys. Rev. Lett. **70**, 2008 (1993); Y. De Wilde *et al.*, *ibid.* **72**, 2278 (1994).
[20] B. S. Shivaram, T. F. Rosenbaum, and D. G. Hinks, Phys. Rev. Lett. **57**, 1259 (1986).
[21] C. H. Choi and J. A. Sauls, Phys. Rev. Lett. **66**, 484 (1991).
[22] K. A. Park and R. Joynt, Phys. Rev. Lett. **74**, 4734 (1995).
[23] G. Yin and K. Maki, Physica B **199-200**, 224 (1994).
[24] Simply replacing k_i by v_i does not lead to orthogonal functions, so higher L harmonics should be orthogonalized to lower L harmonics of the same group representation. For simplicity, we do not use these more complicated functions here.
[25] M. R. Norman, Phys. Rev. Lett. **72**, 2077 (1994).
[26] In this paper, results from a relativistic linearized muffin-tin orbital calculation (with combined corrections and basis functions through $l=3$ on both U and Pt sites) were used.
[27] G. Lehmann and M. Taut, Phys. Status Solidi B **54**, 469 (1972).
[28] First-principle eigenvalues were calculated on a 721 k-point grid in the irreducible (1/24) of the Brillouin zone. These were then fit using a 2541 function Fourier spline series, which allows eigenvalues to be determined at any k point, with velocities being constructed by simple differencing. The Fermi-surface integrals were performed with a linear tetrahedron method, with the zone broken down 72×8^n times. Most calculations used an n of 5, but some were done at an n of 6 to check for convergence.
[29] In general, these functions will be multiplied by a constant (determined by solving the gap equations) which can vary from band to band. In this paper, we take this constant to be independent of band index.
[30] V. Ambegaokar and A. Griffin, Phys. Rev. **137**, A1151 (1965).
[31] H. Monien, K. Scharnberg, L. Tewordt, and D. Walker, Solid State Commun. **61**, 581 (1987).
[32] P. J. Hirschfeld, P. Wolfle, and D. Einzel, Phys. Rev. B **37**, 83 (1988).
[33] B. Arfi, H. Bahlouli, and C. J. Pethick, Phys. Rev. B **39**, 8959 (1989).
[34] L. Coffey, T. M. Rice, and K. Ueda, J. Phys. C **18**, L813 (1985).
[35] C. J. Pethick and D. Pines, Phys. Rev. Lett. **57**, 118 (1986).
[36] S. M. Quinlan, D. J. Scalapino, and N. Bulut, Phys. Rev. B **49**, 1470 (1994).
[37] Y_{54} does not mix with Y_{32} in axial symmetry.
[38] P. A. Lee, Phys. Rev. Lett. **71**, 1887 (1993).
[39] M. J. Graf, S.-K. Yip, J. A. Sauls, and D. Rainer (unpublished).
[40] The analysis in this paper was greatly facilitated by the analytic nature of the basis functions. Most microscopic models, such as the one in Ref. 25, are numerical and thus more difficult to treat given the large number of tetrahedra needed in the zone integrations.